Scientific Research Publishing

World Journal of Condensed Matter Physics, 2024, 14, 21-33
https://www.scirp.org/journal/wjcmp
ISSN Online: 2160-6927
ISSN Print: 2160-6919

Discussion on the Application Prospect of the Transient Electromagnetic Method Based on the Dual Launcher and Mine Advanced Detection

Zhen Yang[1], Huizhou Liu[2*], Shengqing Wang[1], Yu Cao[2], Ya Dong[2], Chenghu Niu[1], Weiwen Song[2], Guoxin Xie[1]

[1]State Grid Energy Hefeng Coal Power Co. Ltd., Tacheng, China
[2]Anhui Huizhou Geology Security Institute Co. Ltd., Hefei, China
Email: *1976293728@qq.com

How to cite this paper: Yang, Z., Liu, H.Z., Wang, S.Q., Cao, Y., Dong, Y., Niu, C.H., Song, W.W. and Xie, G.X. (2024) Discussion on the Application Prospect of the Transient Electromagnetic Method Based on the Dual Launcher and Mine Advanced Detection. *World Journal of Condensed Matter Physics*, **14**, 21-33.
https://doi.org/10.4236/wjcmp.2024.141003

Received: January 9, 2024
Accepted: February 24, 2024
Published: February 27, 2024

Abstract

The dual transmitter implements the equivalent anti-magnetic flux transient electromagnetic method, which can effectively reduce the scope of the transient electromagnetic detection blind area. However, this method is rarely reported in the detection of pipelines in urban geophysical exploration and the application of coal mines. Based on this, this paper realizes the equivalent anti-magnetic flux transient electromagnetic method based on the dual launcher. The suppression effect of this method on the blind area is analyzed by physical simulation. And the detection experiment of underground pipelines is carried out outdoors. The results show that the dual launcher can significantly reduce the turn-off time, thereby effectively reducing the impact of the blind area on the detection results, and the pipeline detection results verify the device's effectiveness. Finally, based on the ground experimental results, the application prospect of mine advanced detection is discussed. Compared with other detection fields, the formation of blind areas is mainly caused by the equipment. If the dual launcher can be used to reduce the blind area, the accuracy of advanced detection can be improved more effectively. The above research results are of great significance for improving the detection accuracy of the underground transient electromagnetic method.

Keywords

A Dual Launcher, Transient Electromagnetic Method, Detection Blind Area, Physical Simulation, Application Prospect, Mine Geophysical Prospecting

1. Introduction

The transient electromagnetic method has been widely used in the exploration of metals, coalfields, oil and gas, and other mineral exploration and engineering environment exploration because of its light equipment, high construction efficiency, small terrain impact, no grounding conditions, and strong resolution. However, due to the electromagnetic coupling of early data, there is a "blind area" in shallow detection, and the depth range of the blind area is usually the key area in engineering investigation, which is easy to affect the exploration effect [1]. The equivalent reverse flux transient electromagnetic method (OCTEM) solves the problem that the early signal of the transient electromagnetic method is affected by mutual inductance, avoids the blind area of shallow detection, and has been widely used in industry.

The induced electromotive force of the receiving coil itself is due to the non-zero magnetic flux of the primary field of the receiving coil, which is caused by the change of the magnetic flux after the primary field is turned off. Therefore, only the magnetic flux of the primary field in the receiving coil before and after the break remains unchanged and can be eliminated [2]. Based on this principle, Xi *et al.* [1] proposed the equivalent anti-magnetic flux transient electromagnetic method. This method uses two identical coils with upper and lower parallel coaxial passes with reverse current as the transmitting source, and on the primary field zero magnetic flux plane synthesized by the two coil sources, the pure secondary field coupled to the center of the ground is measured. The launcher can also be called a dual launcher, which is a new method to detect the underground pure secondary field. This method is widely used in industrial fields, such as urban shallow geophysical exploration [3] [4], metal ore field [5] [6], underground karst caves [7] [8] [9] [10], exploration of various goaves [11] [12] [13], exploration of underground disasters [14] [15] and other related fields. However, this method is rarely reported in the detection of pipelines in urban geophysical exploration and the application of coal mines.

Based on this, we realized the equivalent anti-magnetic flux transient electromagnetic method based on the dual launcher. The suppression effect of the method on the blind area was analyzed by physical simulation. The detection experiment of underground pipelines was carried out outdoors to verify the effectiveness of the algorithm. Based on the results of ground experiments, the application prospect of advanced detection in coal mines was discussed, which provided theoretical guidance for improving the detection accuracy of the underground transient electromagnetic method.

2. Principle

2.1. The Formation of the Detection Blind Area

The transient electromagnetic emission coil is a non-pure resistive load. In the actual work process, the emission current needs a certain time to turn off, so that the primary field and the secondary field are mixed, and the early secondary

field cannot be identified. The shallow geological information is mainly reflected by early signals, thus forming a detection blind area. The minimum detection distance of transient electromagnetic detection is the earliest penetration distance that can identify useful signals. It is expressed by $h_{\min}$. In the process of transient electromagnetic detection, the turn-off of the primary field takes a certain amount of time, which is the turn-off time (see Figure 1). The smaller the turn-off time t_{sd} is, the smaller the minimum resolvable depth is. The expression is:

$$h_{\min} = \sqrt{t_{sd}\rho} \tag{1}$$

The inductance and resistance of the loop device can be estimated. The specific formula is as follows:

$$t_{sd} \approx L/R \tag{2}$$

R represents the loop resistance, and L represents the loop inductance. For the resistance R of the wire, there are:

$$R = \rho l/s \tag{3}$$

ρ represents the resistivity, l represents the length of the wire, and s represents the cross-sectional area of the wire. For circular coils, there are:

$$R = \frac{2na}{b^2} \tag{4}$$

where a represents the radius of the coil, b represents the cross-sectional area of the wire, and n represents the number of turns of the coil.

2.2. Working Principle of Dual Launcher Based on Equivalent Anti-Magnetic Flux Transient Electromagnetic Method

Different from the traditional transient electromagnetic method, the equivalent reverse flux transient electromagnetic method (OCTEM) uses a double coil source for transmission. In the case of double dipole excitation source emission, the two transmitting coils produce electromagnetic fields of equal size and opposite directions (as shown in Figure 2).

At the same time, a current I of the same size and opposite direction is supplied to the dual coil source Tx, and the measurement is carried out after the current is turned off. The magnetic field line at the receiving coil is in the horizontal direction. Before and after turning off, its vertical magnetic field is 0, and the magnetic flux in that position plane is 0, while there is a vertical magnetic field in other planes. As shown in Equation (2), the turn-off time is mainly affected by the coil inductance. Therefore, reducing the coil inductance can effectively reduce the turn-off time, thereby reducing the "blind spot" and achieving the goal of detecting shallow underground spaces. The inductance expression in the dual emission device is:

$$L = \sum_{i=1}^{2} L_i - \sum_{i=1}^{2}\sum_{j=1}^{2} M_{ij}\left(i \neq j\right) \tag{5}$$

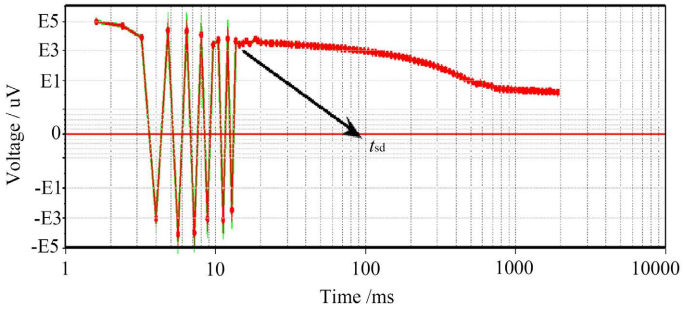

Figure 1. Time-voltage curve.

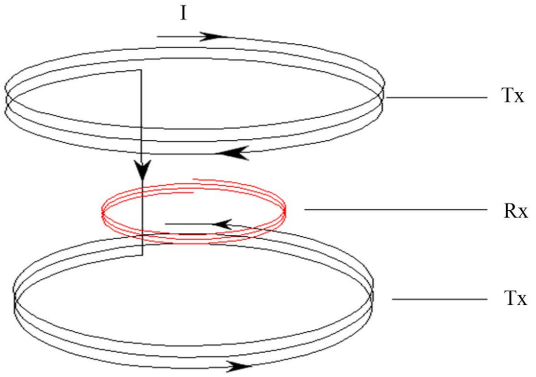

Figure 2. Schematic diagram of the dual launcher.

M_{12} represents the mutual inductance between the first and second return lines. For M_{12} $M_{12}=k\sqrt{L_1L_2}$, in an ideal situation where the coil is tightly wound and no magnetic leakage occurs, $k=1$, which is $M_{12}=L_1$, and in general, $k<1$, which is $0<M_{12}<L_1$. Therefore, the inductance $L<L_1<L_2$ of the dual emission device coil can effectively reduce the inductance, thereby achieving the effect of reducing the blind spot.

According to Maxwell's equations, when the excitation is an oblique step field source, the $R'(t)$ expression of the response of the oblique step transient electromagnetic field can be obtained according to the Duhamel integral:

$$R'(t)=\frac{1}{t_{sd}}\int_0^t R(\boldsymbol{r})\mathrm{d}\boldsymbol{r}\quad(0<t<t_{sd}) \tag{6}$$

$$R''(t)=\frac{1}{t_{sd}}\int_{t-t_{sd}}^t R(\boldsymbol{r})\mathrm{d}\boldsymbol{r}\quad(t>t_{sd}) \tag{7}$$

where (6) and (7) are the induction section and the attenuation section respectively, t_{sd} is the turn-off time, $R(\boldsymbol{r})$ is the transient response excited by the step field source, and r is the substitution function.

According to the symmetry of the electromagnetic field, it can be seen that the vertical components cancel each other out. Therefore, the magnetic field response $H_x(t)$ at the midpoint of the receiving loop of the transmitting-receiving device is:

$$H_x(t)=2A\left[3\varphi(u)-\sqrt{\frac{2}{\pi}}\left(u^2+3\right)u^{-u^2/2}\right] \tag{8}$$

where $A = mal/4\pi r_0^5$ (m is the magnetic moment of a single transmitting coil a is the distance from the receiving point to the axis of the transmitting loop; $2l$ is the distance between the center points of the two transmitting loops; r_0 is the absolute distance $r_0 = \sqrt{a^2 + l^2}$ from the midpoint of the receiving loop to the midpoint of the transmitting loop); $u = \sqrt{\mu_0 r_0^2 / 4\rho t}$ (μ_0 is the vacuum permeability, ρ is the density).

We bring (8) into (6) and (7), the induction section and the attenuation section are obtained as follows:

$$\frac{\partial H_x'(t)}{\partial t} = \frac{mal}{2\pi\left(a^2 + l^2\right)^{\frac{5}{2}}} \frac{t}{t_0}\left[\left(3 + u^2\right)\varphi(u) - 3\sqrt{\frac{2}{\pi}} u \mathrm{e}^{-\frac{u^2}{2}}\right] \quad \left(0 < t < t_{\mathrm{sd}}\right) \tag{9}$$

$$\frac{\partial H_x''(t)}{\partial t} = H_1 - H_2 - H_3 + H_4 \quad \left(t > t_{\mathrm{sd}}\right) \tag{10}$$

where:

$$\begin{cases} H_1 = \dfrac{mal}{2\pi\left(a^2 + l^2\right)^{\frac{5}{2}}} \dfrac{t}{t_0}\left(3 + u^2\right)\varphi(u) \\ H_2 = \dfrac{3}{\sqrt{2}} \dfrac{mal}{\pi^{\frac{3}{2}}\left(a^2 + l^2\right)^{\frac{5}{2}}} \dfrac{t}{t_0} u \mathrm{e}^{-\frac{u^2}{2}} \\ H_3 = \dfrac{mal}{2\pi\left(a^2 + l^2\right)^{\frac{5}{2}}}\left(\dfrac{3t}{t_0} - 3 - \dfrac{t}{t_0}u^2\right)\varphi\left(u/\sqrt{1 - t_0/t}\right) \\ H_4 = \dfrac{3\sqrt{2}mal}{2\pi^{\frac{3}{2}}\left(a^2 + l^2\right)^{\frac{5}{2}}} \sqrt{1 - \dfrac{t_0}{t}} u \mathrm{e}^{-\frac{u^2}{2(1 - t_0/t)}} \end{cases} \tag{11}$$

For isotropic, non-ferromagnetic media, the equation of structural properties is:

$$\begin{cases} \boldsymbol{D} = \varepsilon \boldsymbol{E} \\ \boldsymbol{B} = \mu \boldsymbol{H} \\ \boldsymbol{j} = \gamma \boldsymbol{E} \end{cases} \tag{12}$$

At the same time, according to Faraday's law of electromagnetic induction, the induced voltage curve of the receiving loop under the condition of uniform half-space is obtained by the magnetic field strength of the transition section and the induction section:

$$\nabla \times E(t) = -\frac{\partial B(t)}{\partial t} = -\mu \frac{\partial H(t)}{\partial t} \tag{13}$$

3. Physical Test

3.1. Sampling Parameters and Observation System

A measuring line of 40 cm was selected, with a total of 9 measuring points from 1 to 9, and the distance between measuring points was 5 cm. There is a low resis-

tivity anomaly body with a radius of 3 cm below the fourth measuring point. To ensure that the receiving coil was located in the center of the dual device or on the same plane as the central loop transmitter, a circle with a radius of 5 cm was extracted from a circular foam plate of 7.5 cm, and the receiving coil was wound (as shown in Figure 3). The abnormal body was located at 20 cm of the measuring line, which was directly above the middle measuring point. It was a low-resistance sheet abnormal body with a radius of 3 cm. The sampling parameters are shown in Table 1.

3.2. Data Analysis

According to the above physical model, the dual launcher and the traditional launcher were used for comparative acquisition, and the data acquisition of this line was carried out. The voltage curves of the measuring points of the two devices are shown in Figure 4. Figure 4(a) and Figure 4(b) are the voltage curves of the measuring points of the traditional device at shallow (2 cm) and deep (4 cm), respectively. Figure 4(c) and Figure 4(d) are the voltage curves of the measuring points of the dual reflection device at shallow (2 cm) and deep (4 cm). It can be seen from the figure that: 1) The energy received by the central loop device is stronger than that of the dual transmitter. The energy received by the dual launcher is more concentrated than that of the traditional device. 2) When the abnormal body is located at different depths, the signal received by the shallow abnormal body is stronger.

Figure 3. Model diagram; (a) Self-made equipment diagram; (b) Anomaly location map.

Table 1. Collection parameters of different launch devices.

Parameter	Traditional launch device	Dual emission device
Transmission frequency	125 Hz	125 Hz
Sampling frequency	1.25 MHz	1.25 MHz
Stack number	128	128
Number of tracks	100	100
Measurement point spacing	5 cm	5 cm
Abnormal body radius	3 cm	3 cm
Distance between transmitting coils	0	5 cm

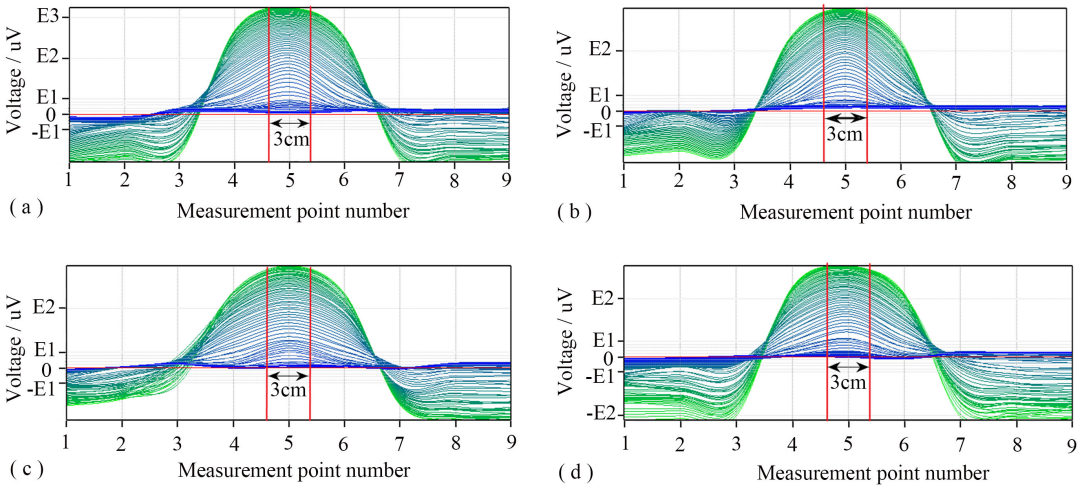

Figure 4. Measuring point voltage curve; (a) The voltage curve of the shallow (h = 2 cm) measuring point under the traditional device; (b) The voltage curve of the deep (h = 4 cm) measuring point under the traditional device; (c) the voltage curve of the shallow (h = 2 cm) measuring point under the dual launcher; (d) The voltage curve of the deep (h = 4 cm) measuring point under the dual launcher.

To further analyze the suppression effect of the dual device on blind spots, shallow time-voltage signals were extracted from the fifth measuring point at the same depth, and the results are shown in **Figure 5**. **Figure 5(a)** was the traditional device receiving the shallow fifth measuring point time-voltage diagram, and **Figure 5(b)** was the dual launcher receiving the shallow fifth measuring point time-voltage diagram.

As shown in the figure, the signal strength of traditional transmission devices is significantly stronger than that of dual transmission devices, but the shutdown time of traditional transmission devices is between 10 μs and 20 μs, and the shutdown time of the dual emission device is less than 10 μs. Compared to traditional devices, the use of dual emission devices reduces the turn-off time and blind spots while losing some of the received signal strength. Therefore, compared to traditional emission device forms, dual emission devices have better detection effects for shallow or ultra-shallow layers. The reason why the theoretical complete elimination result was not achieved in this experiment is that the receiving coil Rx of the dual transmitting device did not reach the theoretical center of the two transmitting coils Tx.

4. Field Detection

4.1. Site Layout

In this field experiment, the dual launcher and traditional reflection were used to detect the underground known metal fire water supply pipe. The diameter of the metal pipeline was 0.2 m, the buried depth of the pipeline was 1.0 m, the soil filling layer was covered above the pipeline, and the surface asphalt road was covered. A survey line was arranged in the vertical direction of the pipeline, and the dual transmitter and traditional reflection were used for detection. The field

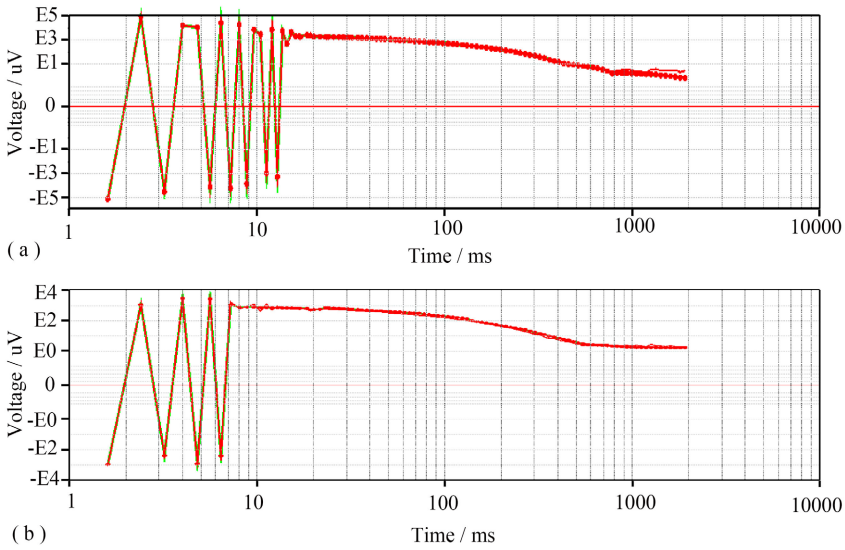

Figure 5. Time-voltage diagram; (a) The traditional device receives the time-voltage diagram of the shallow fifth measuring point; (b) The time-voltage diagram of the fifth measuring point of the dual launcher receiving the shallow part.

layout is shown in **Figure 6**, where **Figure 6(a)** is the position and direction of the metal pipeline, and **Figure 6(b)** is the target pipeline position.

The radius of the transmitting coil used was 0.5 m, the number of turns of the coil was 10, and the distance between the two coils of the dual transmitting device was 0.05 m. The radius of the receiving antenna coil was 0.48 m, and the number of coil turns was 15. The receiving antenna was located in the middle of the two coils of the dual transmitter. Comparative experiments were carried out using dual launchers and traditional launchers.

4.2. Analysis of Detection Results

The time-voltage curve of different measuring points is shown in **Figure 7**, which is obtained when the coil is directly above the pipeline. The blind area suppression range of the two devices is analyzed by the difference of the turn-off time of the two methods, to analyze the suppression effect of the dual reflection device on the blind area. Where t_1 and t_2 represent the turn-off time of the dual launcher and the traditional launcher, respectively. It can be seen from **Figure 7** that the comparison of the turn-off time is $10 < t_1 < t_2$. Therefore, compared with the traditional launcher, the range of the blind area of the dual launcher is relatively small.

To further analyze the detection effect of the dual launcher device, the data are processed to obtain the apparent resistivity profile results. As shown in **Figure 8, Figure 8(a)** is the apparent resistivity profile of the conventional device, and **Figure 8(b)** is the apparent resistivity profile of the dual launcher. The negative sign of the ordinate in the graph indicates the underground depth. It can be seen from the figure that the low resistance anomaly displayed by the traditional device is relatively wide, and the low resistance anomaly displayed by the dual launcher

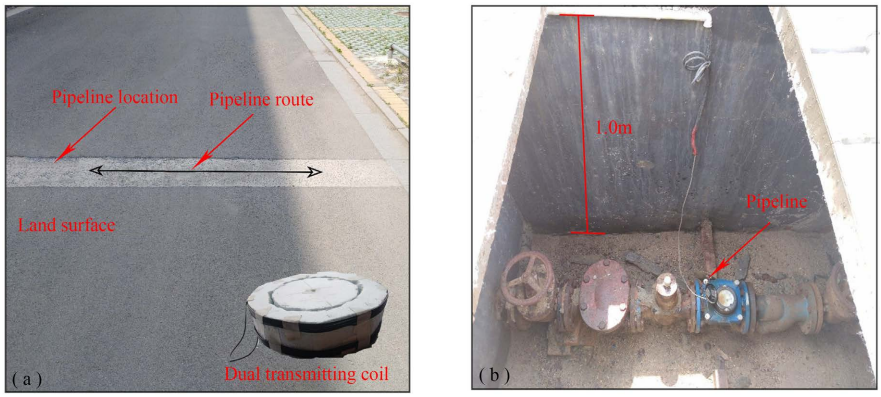

Figure 6. The scene situation; (a) the position and direction of the metal pipe; (b) the Target pipe position.

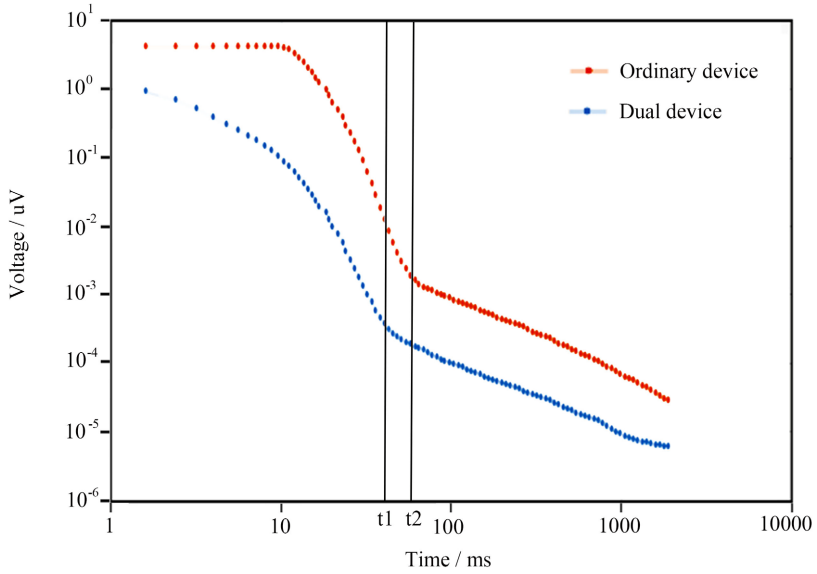

Figure 7. Time-voltage curves directly above the pipeline under different device types.

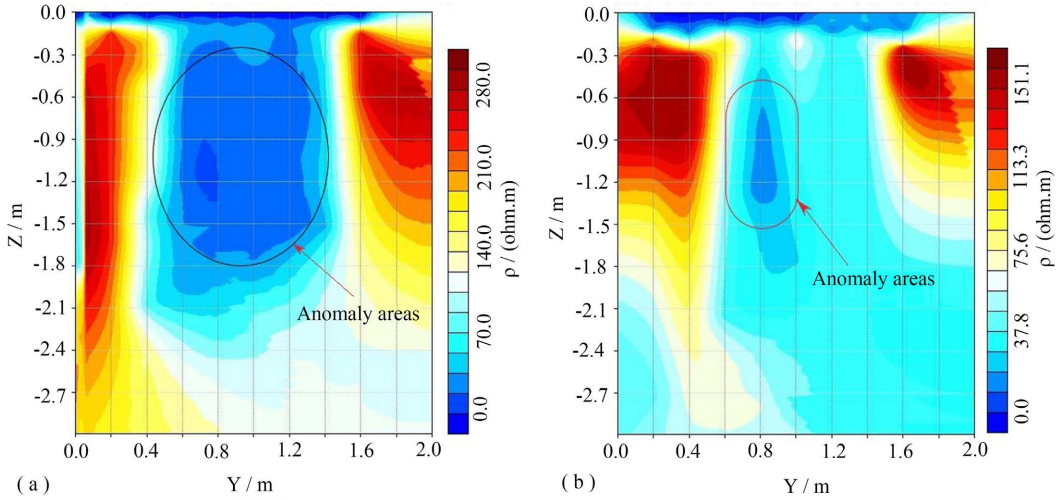

Figure 8. Result chart; (a) The apparent resistivity profile of conventional device; (b) Apparent resistivity profile of dual launcher.

is relatively narrow, and the range of the blind area is relatively small. The blind area of the traditional launcher was connected with the abnormal area, which had a great influence on the interpretation of the data. Combined with the actual situation, the measured pipeline was located directly below Y = 0.8 m, the pipeline diameter was 0.2 m, and the buried depth of the pipeline was 1.0 m. Therefore, the longitudinal and lateral resolution of the dual launcher was relatively high, and the position and size of the measured pipeline were more accurate.

5. Preliminary Discussion on the Application of the Transient Electromagnetic Method of the Dual Transmitter in Mine Advanced Prediction

The transient electromagnetic method is also one of the commonly used geophysical prospecting methods in coal mines. Due to the limitations of the underground construction environment, it is impossible to adopt the form of a large coil device, and only a multi-turn small coil with a side length of less than 3 m can be adopted. The underground transient electromagnetic method has certain directional characteristics in the construction process. During the detection process, the angle between the emission wire frame and the coal seam floor can be adjusted according to the different geological tasks. Coal roadway excavation is the hardest hit area of the accident [16]. The methods of advanced detection of mine roadways mainly include the seismic wave method [17], a direct current method [18], a transient electromagnetic method [19], and other geophysical methods. With the requirements of safe production, the transient electromagnetic method has gradually become the mainstream method. However, the current treatment of blind area elimination in the minefield has been reported. The reason is that the roadway environment is complex, there are various metal support environments around, and the interference is relatively large. At this time, although the dual launcher can eliminate its primary field, it cannot deal with the interference problems caused by surrounding metals (detection of goaf [20] [21], detection of roof water damage [22] [23], detection of hidden water-bearing collapse columns and water-conducting fracture zones [24] [25] and other fields). The interference in front of roadway excavation is relatively small, and the formation of blind areas is mainly caused by the equipment itself. If the dual transmitter can be used to reduce the range of blind area, the accuracy of advanced detection can be improved more effectively, which can provide an effective guarantee for the safe excavation of the roadway.

6. Conclusion

To effectively reduce the blind area of transient electromagnetic detection, the equivalent anti-magnetic flux transient electromagnetic method is realized by using the dual launcher, which can effectively reduce the influence of the detection blind area. However, this method is rarely reported in the detection of pipelines in urban geophysical exploration and the application of coal mines. Based

on this, we realized the equivalent anti-magnetic flux transient electromagnetic method based on the dual launcher. The suppression effect of this method on the blind area is analyzed by physical simulation. The detection experiment of underground pipelines was carried out outdoors. The results showed that the dual launcher can significantly reduce the turn-off time, thereby effectively reducing the impact of the blind area on the detection results, and the pipeline detection results verify the device's effectiveness. Based on the ground experimental results, the application prospect of my advanced detection is discussed. Compared with other detection fields, the formation of blind areas is mainly caused by the equipment. If the dual launcher can be used to reduce the blind area, the accuracy of advanced detection can be improved more effectively. The above research results are of great significance for improving the detection accuracy of the underground transient electromagnetic method.

The raw data collected by transient electromagnetic in this article exhibits varying degrees of signal fluctuations in both the primary and late secondary fields. The main reasons for this situation are 1) excessive matching resistance of the receiving coil; and 2) When there is severe interference from celestial and human factors, noise may remain in the data after periodic superposition. Therefore, to improve the data quality of the dual launch device and enhance the detection accuracy of the dual launch device for shallow targets, the time window pumping and period stacking processing for the dual launch device is an important direction for subsequent research on transient electromagnetic data processing.

Acknowledgements

This paper is supported by the National Natural Science Foundation of China (Nos. 41974149).

Conflicts of Interest

The authors declare no conflicts of interest regarding the publication of this paper.

References

[1] Xi, Z.Z., Long, X., Zhou, S., Huang, L., Song, G., Hou, H.T. and Wang, L. (2016) Opposing Coil Transient Electromagnetic Method for Shallow Subsurface Detection. *Chinese Journal of Geophysics*, **59**, 3428-3435.

[2] Huang, W., Hu, Y., Zhu, J., Cen, Z. and Bao, J. (2022) The Measurement and Evaluation of the Electromagnetic Environment from 5G Base Station. *Detection*, **9**, 1-11. https://doi.org/10.4236/detection.2022.91001

[3] Wang, B.Z., Li, C.X., Qiu, B., Liu, L., Zhou, S.C., Ma, X.F., Wang, J.J. and Guo, G.Y. (2021) Application of Equivalent Anti-Magnetic Flux Transient Electromagnetic Method in Fine Detection of Urban Karst. *Resources Environment and Engineering*, **35**, 727-732.

[4] Wang, L., Long, X., Wang, T.T., Xi, Z.Z., Chen, X.P., Zhong, M.F. and Dong, Z.Q.

(2022) Application of the Opposing-coil Transient Electromagnetic Method in Detection of Urban Shallow Cavities. *Geophysical and Geochemical Exploration*, **46**, 1289-1295.

[5] Kuang, J.J., Wang, H. and Liu, J.H. (2020) Application of Equivalent Anti Magnetic Flux Transient Electromagnetic Method in the Exploration of a Certain Lead-Zinc Deposit. *West-China Exploration Engineering*, **32**, 139-142.

[6] Xiao G., Lian, W.Z. and Ma, D.X. (2021) Application of Equivalent Anti Magnetic Flux Transient Electromagnetic Method in the Detection of Polymetallic Deposits. *Gansu Science and Technology*, **37**, 34-35+40.

[7] Wang, Y., Xi, Z.Z., Jiang, H., Hou, H.T., Zhou, S. and Fan, F.L. (2017) The Application Research on the Detection of Karst Disease of Airport Runway Based on OCTEM. *Geophysical and Geochemical Exploration*, **41**, 360-363.

[8] Li, Y.N. (2017) The Application of Equivalent Anti Magnetic Flux Transient Electromagnetic Method in the Detection of Cave Deposits. *Railway Investigation and Surveying*, **43**, 96-98.

[9] Yang, J.M., Wang, H.C. and Sha, C. (2018) An Analysis of Karst Exploration Based on Opposing Coils Transient Electromagnetic Method. *Geophysical and Geochemical Exploration*, **42**, 846-850.

[10] Xie, J. Liu, Y., Li, X.Q., Lu, Y.L. and Li, G.L. (2021) The Application of Opposing Coils Transient Electromagnetics in the Detection of Karst Subsidence Area. *Coal Geology & Exploration*, **49**, 212-218+226.

[11] Xin, J. (2019) The Application of Opposing Coil Transient Electromagnetic Method to Detect Shallow Goaf. *Chinese Journal of Engineering Geophysics*, **16**, 718-722.

[12] Gao, Y. (2019) The Application Effect on Detecting Goaf of Gypsum Mine by Opposing Coils Transient Electromagnetics Method. *Geophysical and Geochemical Exploration*, **43**, 1404-1408.

[13] Jiang, Z.X., Xu, Y., Aisikaer, T., Kong, F.L. and Ling, F. (2023) The Application of Opposing Coils Transient Electromagnetic in Mined out Area Detection in Coalfield. *Chinese Journal of Engineering Geophysics*, **20**, 163-170.

[14] Peng, X.L., Xi, Z.Z., Wang, H., Shen, J.P., Hou, H.T. and Gao, Y. (2018) Comparison of Application of Equivalent Anti Magnetic Flux Transient Electromagnetic Method in Geological Hazard Detection. *West-China Exploration Engineering*, **30**, 147-150+153.

[15] Zhou, X.F. (2019) Application of equivalent Anti Magnetic Flux Transient Electromagnetic Method in Geological Hazard Detection. *China Metal Bulletin*, No. 5, 259-260.

[16] Cheng, J.L. Li, F., Peng, S.P. and Sun, X.Y. (2014) Research Progress and Development Direction on Advanced Detection in Mine Roadway Working Face Using Geophysical Methods. *Journal of China Coal Society*, **39**, 1742-1750.

[17] Zhang J. (2020) Study on the Mine Multi-Wave Scattering Imaging Method and Its Application. China University of Mining and Technology, Xuzhou.

[18] Liu, S.D., Liu, J. and Yu, J.H. (2014) Development Status and Key Problems of Chinese Mining Geophysical Technology. *Journal of China Coal Society*, **39**, 19-25.

[19] Jiang, Z.H., Yue, J.H. and Liu, Z.X. (2007) Application of Mine Transient Electromagnetic Method in Forecasting Goaf Water. *Chinese Journal of Engineering Geophysics*, **4**, 291-294.

[20] Chang, J.H. Yu, J.C. and Liu, Z.X. (2016) Three-Dimensional Numerical Modeling of Full-Space Transient Electromagnetic Responses of Water in Goaf. *Applied*

Geophysics, **13**, 539-552+581-582. https://doi.org/10.1007/s11770-016-0572-y

[21] Liu, P.X., Xu, G.Y., Cao, W.K., Gao, F., Cui, H.Y. and Zhen, Z.Q. (2020) Application of Transient Electromagnetic Detection in Underground Water-Rich Air Goaf. *Coal and Chemical Industry*, **43**, 49-51.

[22] Li, Y. and Yu, J.C. (2005) Research on Transient Electromagnetic Exploration Technology for Mining Face Roof with High Water Content in Mines. *Energy Technology and Management*, **3**, 15-16.

[23] Yu, J.C., Liu, Z.X., Tang, J.Y. and Wang, Y.Z. (2007) Transient Electromagnetic Detecting Technique for Water Hazard to the Roof of Fully Mechanized Sub-Level Caving Fac. *Journal of China University of Mining & Technology*, **36**, 542-546.

[24] Li, X.X. (2023) Study on Response Characteristics and Application of Mine Transient Electromagnetic Monitoring. China University of Mining and Technology, Xuzhou.

[25] Xing, X.J. (2019) Mine Transient Electromagnetic Fixed Point Three-Dimensional Advance Detection Technology. *Safety in Coal Mines*, **50**, 67-71+75.